J. Fluid Mech. (1969), *vol.* 39, *part* 4, *pp.* 735–752
Printed in Great Britain

The effect of base bleed on the steady separated flow past bluff objects

By L. G. LEAL† AND A. ACRIVOS
Department of Chemical Engineering, Stanford University

(Received 17 March 1969)

The modifying effect of base bleed on the steady separated flow past a two-dimensional bluff body is considered. Detailed experimental results are presented for Reynolds numbers R between 50 and 250 and for bleed coefficients b in the range 0 to 0·15. The streamline pattern near the object is found to be strongly affected by small changes in the rate of bleed, with the recirculating closed wake disappearing altogether for $b > 0{\cdot}15$. Nevertheless, the qualitative dependence on R of the physical dimensions of the near-wake region and the associated streamwise pressure profile appear to be unaffected by base bleed.

1. Introduction

The possibility of designing airfoils having bluff trailing edges has attracted considerable attention in recent years for, as pointed out by Nash (1962) and others, such airfoils can have lower drags at supersonic and transonic speeds than those with conventional long, tapering rear sections, owing, principally, to the elimination of wave drag. At subsonic speeds, however, the overall drag is greatly increased as a result of the form drag associated with the presence of separation at the trailing edge. Hence, a number of recent investigations have dealt with various means of interfering with the unsteady flow in the wake so as to reduce this form drag. One such mode of interference, most recently studied by Bearman (1967) and by Wood (1967), is known as base bleed, and involves the injection of relatively low velocity fluid through the trailing edge base of the airfoil.

Wood's (1967) work consisted primarily of an experimental study conducted in a water-filled tow tank at a Reynolds number R of approximately $1{\cdot}7 \times 10^3$ and with base bleed coefficients b ranging from 0 to 0·20, where $R \equiv Uh/2\nu$ and $b \equiv Q/Uh$, with h being the base height, Q the volumetric flow rate of the bleed fluid per unit span width, and U the free stream velocity. Wood concluded that, in this range, an increase in b was accompanied by a marked decrease in the pressure drag, a corresponding downstream displacement of the formation region of the vortex street, and a decay in the vortex strength. For his investigation, Bearman (1967) employed a low-turbulence level wind tunnel facility with $6{\cdot}5 \times 10^3 \leqslant R \leqslant 21 \times 10^3$ and bleed coefficients b between $-0{\cdot}04$ and $+0{\cdot}16$. In addition to the increased distance to vortex formation and increased rear

† Present address: DAMTP, University of Cambridge.

pressure coefficients, Bearman observed that, with increasing b, the shedding frequency of the associated vortex street first increased and then decreased together with the vortex strength until, apparently, the vortices disappeared altogether at $b \sim 0{\cdot}16$.

As a result of his experimental observations, Bearman proposed a qualitative model for the corresponding *steady* flow field, pictured in figure 1, in which the detached shear layers are supposed to entrain, first the bleed fluid, and then (provided b is not too large) some additional fluid which must be supplied from downstream. Thus, according to Bearman, a recirculating eddy should form if the wake region is assumed to be closed.

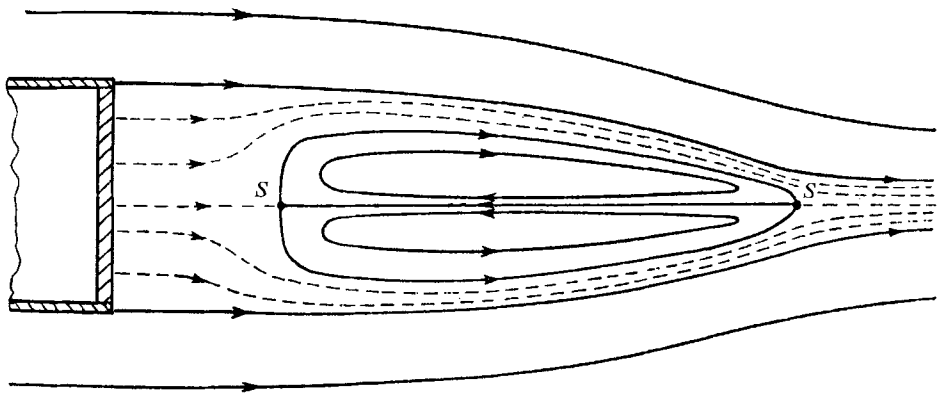

FIGURE 1. Bearman's (1967) model. — → —, bleed air. S, stagnation point.

In the present work, the effect of base bleed on a recirculating wake behind a bluff body was investigated experimentally under conditions such that the shear layer at the separation point was laminar and the flow field *strictly steady*. The streamline pattern in the wake region was observed photographically by means of a bubble-tracer technique; in addition, a number of pertinent quantities, such as the physical dimensions of the wake region, were measured and will be presented.

The primary purpose of this study was not so much to assess the usefulness of base bleed as a practical means for reducing the drag of non-streamlined airfoil sections, but rather, to take advantage of this experimental configuration in order to investigate further the structure of *steady* recirculating wakes at high Reynolds numbers R. Although the Reynolds number must necessarily be limited to maximum values of order several hundred so as to ensure that the wake remain steady, it is believed that the results are indicative of the structure of the *steady* flow field in the *limit* of very high Reynolds numbers. This important point has been discussed at some length in previous communications (Acrivos *et al.* 1964, 1965, 1968). As will be seen presently, the new results to be presented in this paper are completely consistent with those reported earlier by the authors. In addition, they seem to indicate that such basic properties of the near-wake region as its physical dimensions and its streamwise pressure profile are dominated

by the structure of the separated shear layer and the surrounding potential flow, thus maintaining the same qualitative dependence on Reynolds number in the presence of base bleed as was measured with $b \equiv 0$, in spite of the fact that the detailed flow patterns in the wake are considerably changed. A mechanism of wake formation which appears to be consistent with our observations is the so-called entrainment-detrainment model, most recently discussed by Roshko (1967) and briefly by Bearman (1967), according to which the standing eddy behind the body forms as a result of fluid being entrained into the shear layer that exists along the detached streamline.

2. Apparatus and experimental techniques

The experiments were performed in the closed loop oil tunnel described by Acrivos *et al.* (1964, 1965, 1968). Such important features of this system as the two-dimensionality of the basic flow in the test section have been discussed in these publications, as well as more recently by Leal (1969), and thus will not be dealt with further in this paper. In addition, many of the procedures adopted previously were also employed in the present work, so that their description here will be extremely brief. In particular, the characteristic (free stream) velocity U was again chosen as the centreline fluid velocity measured at the position of the test piece under the same operating conditions but without the object, and the reference static pressure was taken as the pressure on the tunnel wall directly beneath the point of measurement. Furthermore, flow visualization was again achieved by time exposure photography of extremely small, entrained air bubbles, with appropriate illumination and depth of field, so that only a vertical section along the centre of the tunnel, 0·5–1 cm in thickness, remained in focus.

The test object, which was positioned midway between the top and bottom walls of the test section, is best described by reference to figure 2. As shown, the upper portion consisted of an elliptic nose followed by a parallel rear section terminating in an open trailing edge which was covered generally by a fine mesh screen and occasionally by a solid metal plate. The flat bottom of the model was extended several inches beyond this edge and was fitted along the centreline with a number of taps which were used to measure the pressure profiles along the recirculating wake. Although this extended surface certainly stabilizes the flow, thus increasing the range of Reynolds number for which a steady, recirculating wake is attained, it has been shown by Acrivos *et al.* (1968) that, for the case of a backward-facing step, the basic features of the near-wake region are otherwise qualitatively unchanged by its presence.

A relatively uniform bleed rate was attained across the whole test section, with the exception of the solid 1·2 cm section at either end, by means of a rectangular manifold built into the interior of the model (see figure 2). This manifold was equipped with removable inserts which served to change the variation of the cross-sectional area with distance so as to produce an effectively uniform outflow spanwise over the full range of bleed rates employed. Preliminary tests in which, with the manifold oriented vertically, the height of the upwelling fluid was measured accurately as a function of position along the face of the manifold,

indicated that overall variations of less than 10% could be achieved over the full range of flow rates used, and that these variations occurred near the ends of the manifold, the centre $\frac{2}{3}$ being essential uniform. Although these measurements were undoubtedly affected by the tendency of the liquid to spread on the face of the manifold, thereby tending to equalize the liquid height, a few spot checks of the assembled apparatus (in the tunnel) showed that the spanwise variations in the flow rate were only slightly larger than those obtained in these preliminary tests. At any rate, Bearman (1967) previously demonstrated that the centre-span properties of the flow field in the wake are quite insensitive to small spanwise non-uniformities of the bleed flow. This was indirectly confirmed in the present work, since changing manifold inserts, while keeping the bleed rate constant, caused no measurable variations in the centre-span properties of the wake in spite of the fact that the detailed non-uniformities of the bleed flow were somewhat altered.

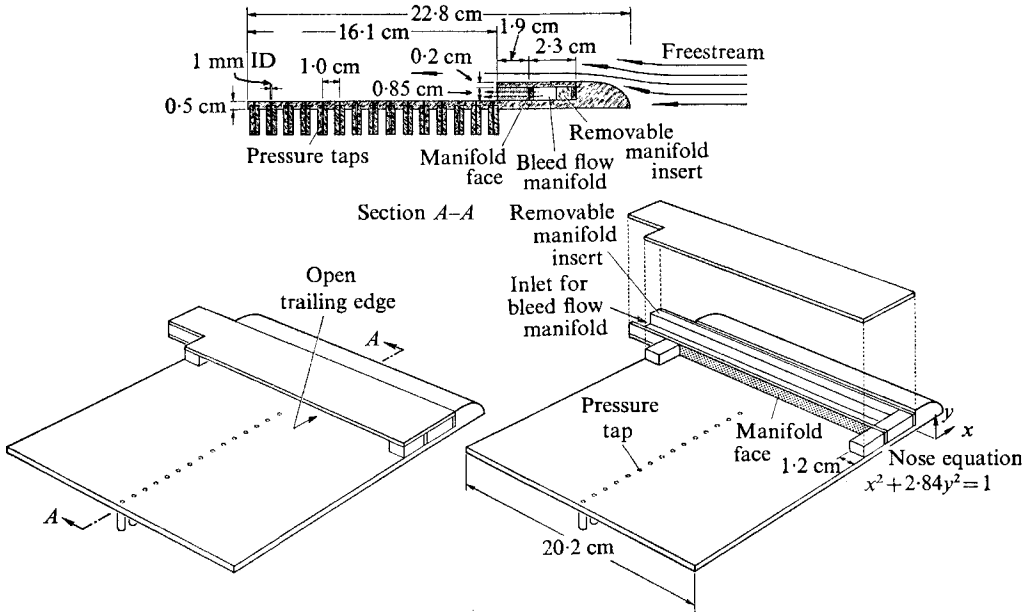

FIGURE 2. The test model.

The 1·9 cm section (see figure 2) between the face of the manifold and the open trailing edge served to equalize further any spanwise variations in the bleed flow. In addition, the extremely fine mesh screen which generally covered the 'open' trailing edge, served to flatten the flow profiles that were built up in this preceding section.

The bleed fluid was fed from an auxiliary tank into the manifold through the the side of the tunnel using a helical rotor gear pump that gave an extremely smooth outflow, and was returned from the tunnel by gravity feed through an overflow valve. The rate of bleed flow was measured by a pair of previously calibrated Fischer and Porter rotameters, whose capacity relative to the actual throughput was such that no reading was less than 30% of full scale. Thus, the

volume flow rate of the bleed stream was estimated to be accurate within $\pm 3\%$. Also, the temperature of the bleed fluid and that of the fluid already in the tunnel were controlled to within $\sim \pm 0{\cdot}5\,^{\circ}\mathrm{C}$ of each other, in order to minimize any undesirable buoyancy effects.

3. Experimental results

(i) *Wake structure in the absence of base bleed*

The structure of the high Reynolds number, steady separated flow past a number of two-dimensional bluff objects has been the subject of several recent experimental investigations which were summarized by Acrivos *et al.* (1968). Briefly, the closed-streamline wake was shown to consist primarily of a region of nearly parallel streamlines of $O(R)$ in length and $O(1)$ in width, in which viscous forces were believed to remain important even as $R \to \infty$. In addition, the rear stagnation point pressure coefficient was found, in every case, to attain a substantially negative constant value for $R > \sim 100$. Based upon these results, a theoretical model was proposed by Acrivos *et al.* (1965) for the high R, asymptotic structure of the closed wake, which requires, in addition, that the streamwise pressure gradient be $O(1/R)$ throughout the major portion of the wake, thus precluding the recovery of the pressure coefficient $\hat{p}$ to its free stream value over distances less than $O(R)$. This feature has recently been confirmed in Acrivos *et al.* (1968) for the case of a backward-facing step.

Since the leading portion of the bluff body shown in figure 2 is considerably more streamlined than that for the majority of the objects studied in (1968), it was felt desirable to confirm that, for $b \equiv 0$, the structure of the near-wake was consistent with that outlined above. Thus, a number of experiments were conducted with $b \equiv 0$, in which a closed-streamline wake-region, similar to that shown in figure 3(*a*), plate 1, was observed.

Using the notation of figure 3(*b*), plate 1, figures 4 and 5 depict the length of the standing eddy and the position of the associated vortex centre as a function of the Reynolds number R, where $R = Ud/\nu$. These were measured from photographs of the flow field, a typical example of which is shown in figure 3(*b*).† As expected on the basis of the experimental results reported in Acrivos *et al.* (1968), the wake length (l_1), and the downstream distance to the vortex centre (l_2) increased linearly with R, for $R > \sim 100$. On the other hand, the maximum wake width always occurred at the trailing edge and thus equalled d, in contrast to the cases studied in (1968), in which this parameter, although independent of R for large Reynolds numbers, was always somewhat larger than the width of the object. Also, as shown in figure 5, the vertical height of the vortex

† In earlier experiments with a backward facing step (see Acrivos *et al.* 1968) the location of the wake stagnation point was also measured directly by viewing through a Graphlex reflex camera the position at which small bubbles, held by buoyancy against the underside of the splitter, remained motionless. Since the two measurements gave comparable results (Leal 1969), it was concluded that the separation and reattachment streamlines shown in the photographs were in fact identical as, of course, should be the case for a two-dimensional flow.

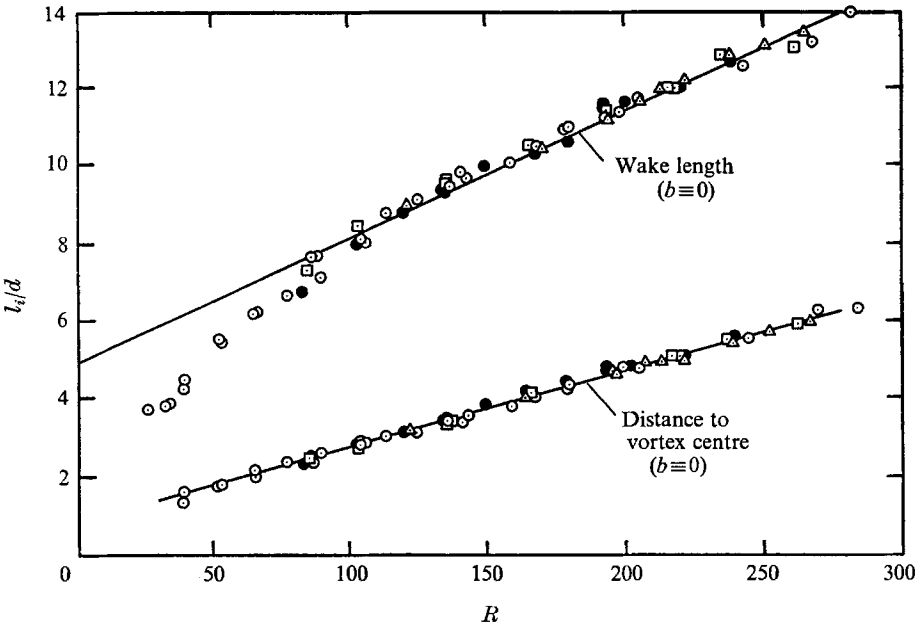

FIGURE 4. The effect of Reynolds number on the wake length and on the streamwise distance to the vortex centre ($b = 0$). ⊙, △ with the trailing base covered by the screen; ⊡, with the trailing-edge base covered by a solid metal plate; ●, with the trailing-edge base left completely open.

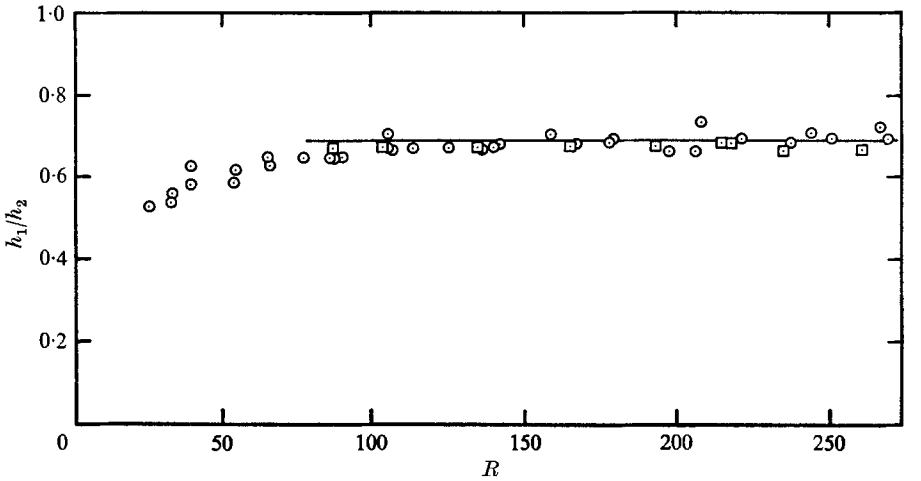

FIGURE 5. The effect of Reynolds number on the vertical height of the vortex centre ($b = 0$). ⊙, with the trailing-edge base covered by the screen; ⊡, with the trailing-edge base covered by a solid metal plate.

centre (h_1) attained for $R > \sim 100$ a constant value of $\frac{2}{3}$ relative to the wake width (h_2) at the same distance from the trailing edge, again in accord with the (1968) results. It may be noted that, in both figures 4 and 5, the data points are not only those for which the trailing edge base was covered by the screen described

previously, but also where it was either covered by a solid metal plate or left completely open. No measurable differences were found to exist between these three cases. In fact, in the latter case, the fluid within the base cavity appeared to remain completely motionless.

Finally, the pressure coefficient $\hat{p} \equiv (\Delta P/(\frac{1}{2}\rho U^2))$ was measured at the base of the trailing edge (see figure 3 (*a*)) and is shown in figure 6 plotted as a function of Reynolds number R. It appears, as expected, that $\hat{p}$ will attain a substantially negative value ($\sim -0{\cdot}5$) even as $R \to \infty$. Although the value of $\hat{p}$, at a fixed R, is somewhat influenced by the finite blockage ratio (approximately equal to 0·05), we believe, bearing in mind the (1968) results, that the qualitative dependence of $\hat{p}$ on R will remain unchanged by further decrease in blockage. Again, as was the case for l_1, l_2 and h_1/h_2, the pressure coefficient at the trailing edge was unaffected by the presence or absence of an open base. This is not surprising since, as was shown in (1968), the fluid in a $O(1)$ region adjacent to the trailing edge becomes stagnant relative to the free stream, as $R \to \infty$. In § 3 (ii), it will be shown that the pressure profile along the wake is independent of R when plotted against (x/l_1), again in agreement with the theoretical model described in (1968).

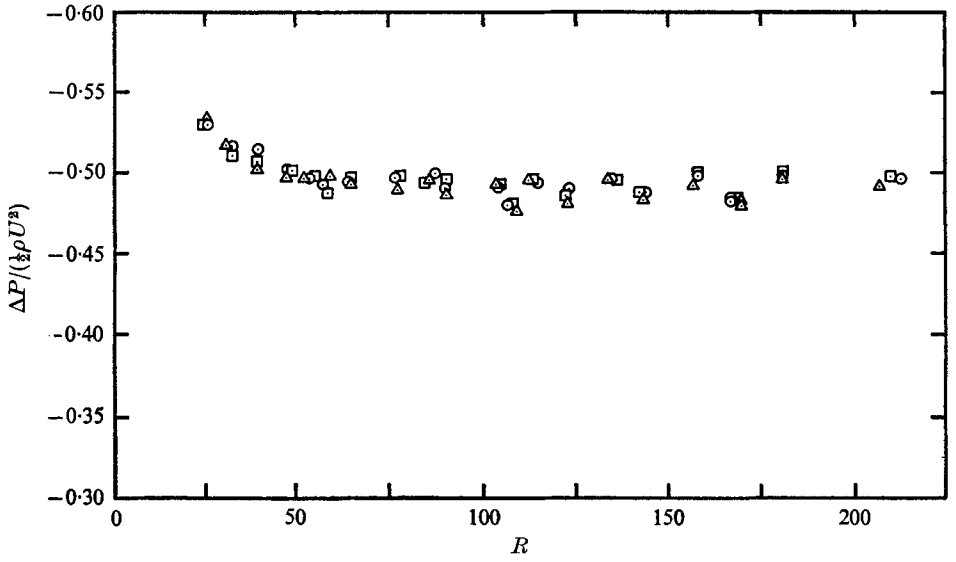

FIGURE 6. The effect of Reynolds number on the rear stagnation point pressure coefficient ($b = 0$). ⊙, with the trailing-edge base covered by the screen; △, with the trailing-edge base covered by a solid metal plate; □, with the trailing-edge base completely open.

It is of some interest now to compare the present results with those given in (1968). For this purpose, we have listed in table 1 the large R relations for the wake length, the wake width and the rear pressure coefficient for a backward-facing step, and the present test-object. Clearly the effect of increasing the forebody bluffness is to increase considerably the wake length and the wake width. In addition, it was observed in the present case that the fluid velocities in the recirculating wake were smaller and that the wake-flow remained steady for

considerably higher values of R than for any of the configurations studied previously. We believe that, except for the change in the wake width, these differences reflect the decrease in the velocity gradients within the separated shear layer which result, at constant R, from the relatively long, streamlined nose section.

	Backward facing step	Present test object
l_1/d	$0{\cdot}27R$	$5{\cdot}0+0{\cdot}032R$
h_2/d	1·8	1·0
$\hat{p}$	−0·64	−0·49

TABLE 1

It is somewhat surprising, at first glance, that the rear pressure coefficients (see table 1) for the step and the present test-object do not differ by as great an amount as would be expected on the basis of a standard potential flow analysis about the forebody and the closed-streamline wake. However, it was indicated in Acrivos *et al.* (1968) that such an analysis, although proper as $R \to \infty$ for objects of finite length, seems to fail when the length of the object is $O(R)$ and its width still kept $O(1)$, as is the case when the closed-streamline wake is included as part of the equivalent body. We believe that this fact may account for the apparent discrepancy between the experimental results and the qualitative prediction of the potential flow analysis. A similar insensitivity of the rear stagnation pressure coefficient to the forebody geometry is apparent in the (1968) results.

In summary, then, the present experimental findings, for $b \equiv 0$, while differing somewhat in detail, show the same qualitative dependence of the basic features of the close streamline wake on Reynolds number as reported in (1968), and thus offer further evidence in support of the theoretical model proposed by Acrivos *et al.* (1965) for the steady, high Reynolds number flow past bluff objects.

(ii) *Effect of base bleed on the structure of steady separated wakes*

A series of photographs of the near-wake, showing the effect at a fixed Reynolds number of increasing the rate of base bleed (i.e. increasing b here defined as Q/Ud with Q being again the volumetric flow rate per unit span width), are presented in figures 7 (*a*)–7 (*d*), plates 2 and 3. Comparing these with figure 1 it is obvious that the flow structure is qualitatively similar to that proposed by Bearman (1967). In addition, with increasing b, the closed streamline region is displaced in the downstream direction while becoming both narrower and shorter. Also, the overall wake-length from the trailing edge to the downstream tip of the reverse flow region appears to decrease slightly. Simultaneously, the velocity of the fluid in the recirculating region decreased markedly, so that even for $b \approx 0{\cdot}12$ it was extremely difficult, with exposure times of 1–2 sec, to observe any motion. For $b > 0{\cdot}15$ the recirculation had effectively disappeared.

Using photographs such as those of figure 7, measurements were made of the position of the vortex centre (l_2, h_1), the downstream distance to the leading

edge of the closed streamline region (l_0) and the overall wake-length (l_1) as defined in figure 7(*e*), plate 3. Shown in figure 8 is the increment in the streamwise distance to the vortex centre (l_2) relative to its value when $b \equiv 0$ (figure 4), for bleed rates $0 < b \leqslant 0{\cdot}12$, and for several fixed values of the Reynolds number in the range $87 \leqslant R \leqslant 262$. The vertical position of the vortex centre as a function of b, for fixed R, is depicted in figure 9. Because of the rather large uncertainty involved in locating the vortex centre in the very slowly recirculating

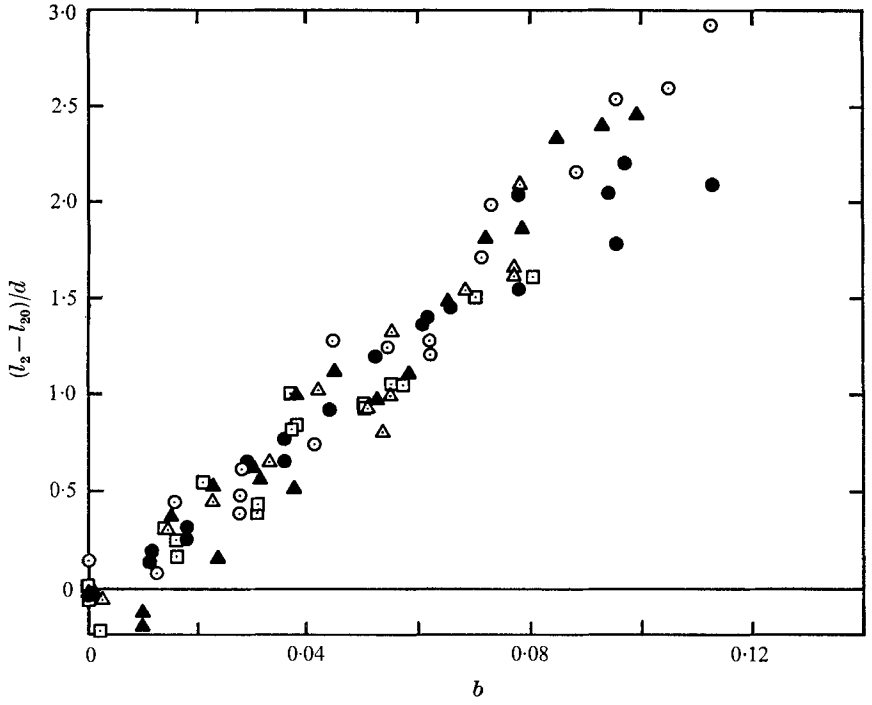

FIGURE 8. The effect of bleed rate on the streamwise distance to the vortex centre. ⊡, $R = 87$; △, $R = 123$; ●, $R = 170$; ⊙, $R = 209$; ▲, $R = 260$. (l_{20} is the value of l_2 at $b = 0$.)

wakes, a rather large scatter of the experimental data was unavoidable. Nevertheless, it appears that, for fixed R, the effect of increasing b is to decrease h_1 while simultaneously increasing l_2, both variations being approximately linearly dependent on b. Furthermore, it is clear that the vertical co-ordinate of the vortex centre (h_1) is independent of R and, since the rate of increase of l_2 with b is independent of R, that the functional dependence of l_2 on R is the same as that observed for $b \equiv 0$, i.e. linear in R for any fixed $b(\leqslant \sim 0{\cdot}12)$.

Similar measurements of the overall wake-length l_1, for various non-zero b and $87 \leqslant R \leqslant 262$, yield figure 10 which depicts the difference between the values of l_1 when $b \neq 0$ and those for $b \equiv 0$ at the same R (figure 4). It is apparent that l_1 decreases slowly with increasing b. Also, as in the case of l_2, l_1 increases linearly with increasing R for any fixed $b(\leqslant 0{\cdot}12)$. Finally, the distance to the

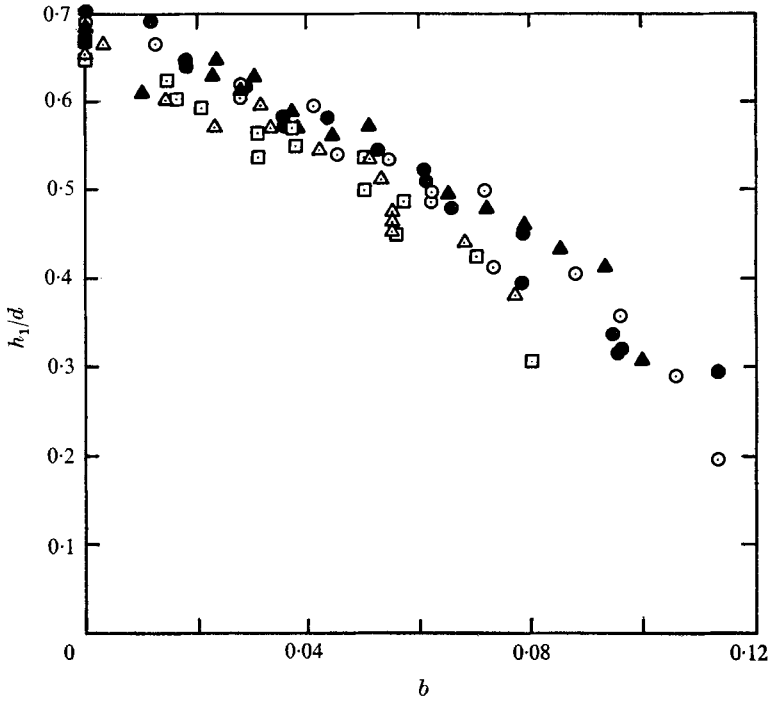

FIGURE 9. The effect of bleed rate on the vertical height of the vortex centre. ⊡, $R = 87$; △, $R = 123$; ●, $R = 170$; ⊙, $R = 209$; ▲, $R = 260$.

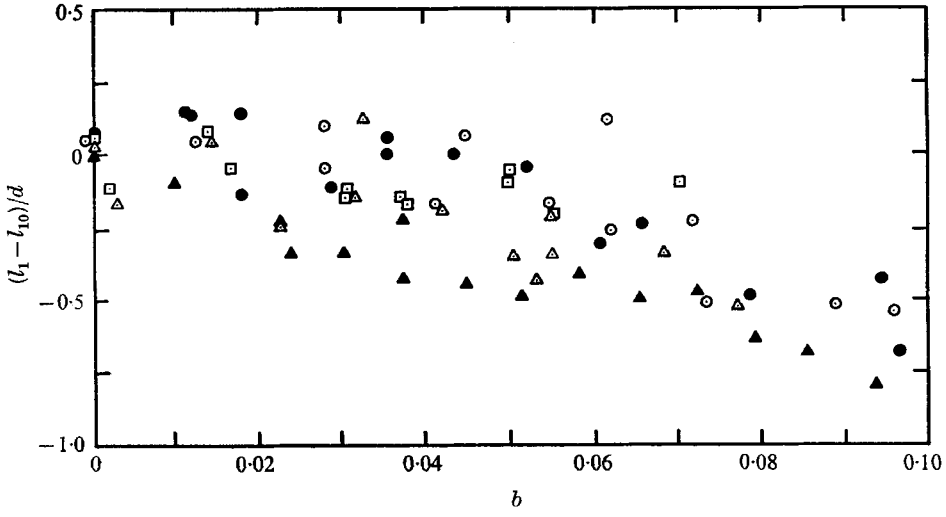

FIGURE 10. The effect of bleed rate on the streamwise distance to the tip of the recirculating region ⊡, $R = 87$; △, $R = 123$; ●, $R = 170$; ⊙, $R = 209$; ▲, $R = 260$. (l_{10} is here and subsequently the value of l_1 at $b = 0$.)

leading edge of the closed-streamline region l_0 was carefully measured as a function of b for fixed R, and the results are shown in figure 11. As noted previously, this distance l_0 was found to increase monotonically with increasing b. The effect of R, for a fixed rate of base bleed, is easily ascertained from figure 12, which was obtained by simply plotting, against R, values of l_0 that were read from the 'best-fit' curves of figure 11 holding b fixed. Thus, within the accuracy of the orginal data, it appears that l_0 varies linearly with R for any fixed $b \leqslant \sim 0{\cdot}10$.

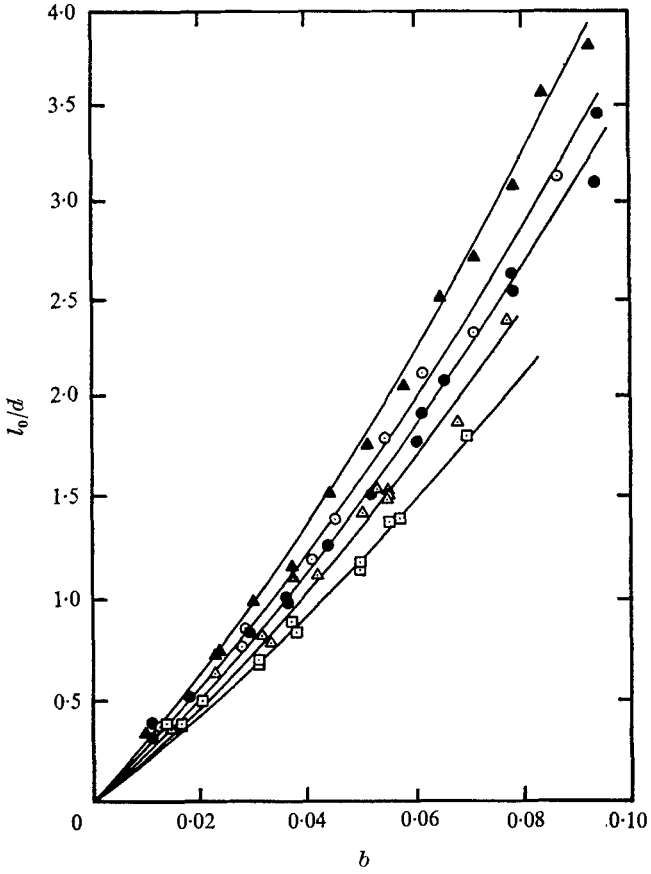

FIGURE 11. The effect of bleed rate on the streamwise distance to the front stagnation point of the recirculating region. ⊡, $R = 87$; △, $R = 123$; ●, $R = 170$; ⊙, $R = 209$; ▲, $R = 260$.

These observations suggest then that, within the accuracy of the data, the characteristic dimensions of the near-wake region for large R are $O(R)$ in the streamwise direction, for fixed b, but $O(1)$ and apparently independent of R along the vertical. Thus, although the detailed structure of the near-wake is obviously more complicated than for the case $b = 0$, the dependence of its physical dimensions on Reynolds number (for high R) appears to remain qualitatively unchanged, at least for small values of $b(\leqslant 0{\cdot}12)$. This, then, would suggest that the asymptotic

model of the wake region for large R, described previously for the case $b \equiv 0$, may be independent of the detailed structure of the flow and, in fact, remain valid even in the presence of base bleed.

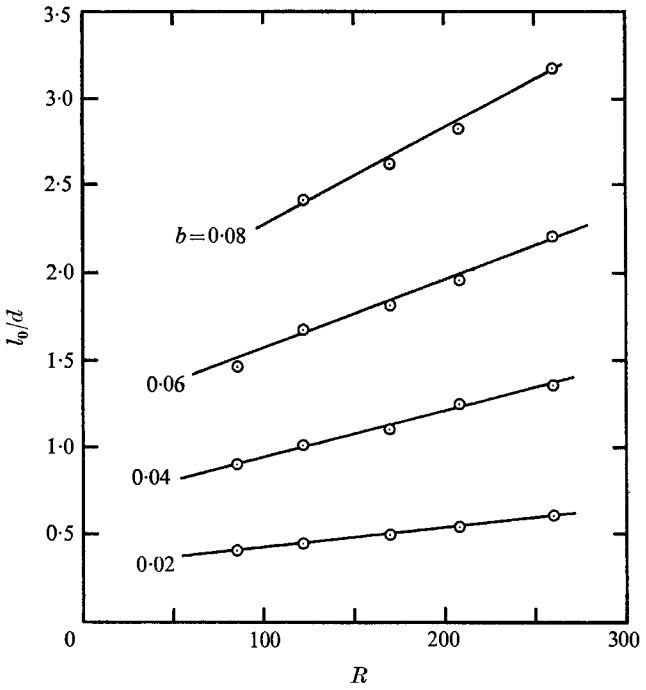

FIGURE 12. The effect of Reynolds number on the streamwise distance to the front stagnation point of the recirculating region.

In order to investigate this point further, a number of measurements were made of the streamwise pressure profile along the centreline of the horizontal plate which, as shown in figure 3, served as the base for the recirculating wake. The results, covering the range $86 \leqslant R \leqslant 226$ and $0 \leqslant b \leqslant 0{\cdot}12$, are depicted in figures 13–16, in which the pressure coefficient is shown as a function of the bleed coefficient b for various downstream distances $\bar{x} = (x/d)$ measured from the trailing edge. It is apparent that, for fixed R, the effect of increasing the bleed rate b is to increase the pressure coefficient in the immediate vicinity of the trailing edge, while simultaneously decreasing the overall rate of pressure recovery. Thus, the measurements at large distances downstream actually led to decreasing values of $\hat{p}$.

If, as was tentatively suggested earlier, the asymptotic structure of the near-wake for large R, described in Acrivos *et al.* (1968) for the case $b = 0$, is to remain valid for non-zero b, then, as also shown there, the pressure coefficient profiles for a fixed value of b and $86 \leqslant R \leqslant 226$ should collapse to a single curve when plotted against an appropriately normalized streamwise distance, linear in R, provided only that the trailing edge base pressure is itself independent of R. In fact, since one of the essential requirements of this asymptotic theory is that, as implied

in §3(i), the pressure coefficient at the trailing edge and at the wake stagnation point be both independent of R, it follows that for $b \equiv 0$, the appropriate characteristic length for normalizing the streamwise distance should be the wake

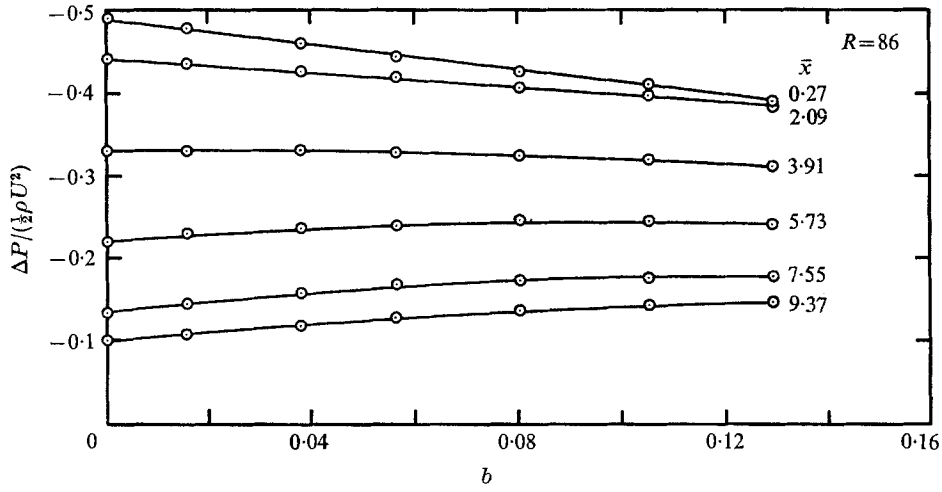

FIGURE 13. The effect of bleed rate on the pressure coefficient along the horizontal base of the model, $R = 86$; $\bar{x} = x/d$.

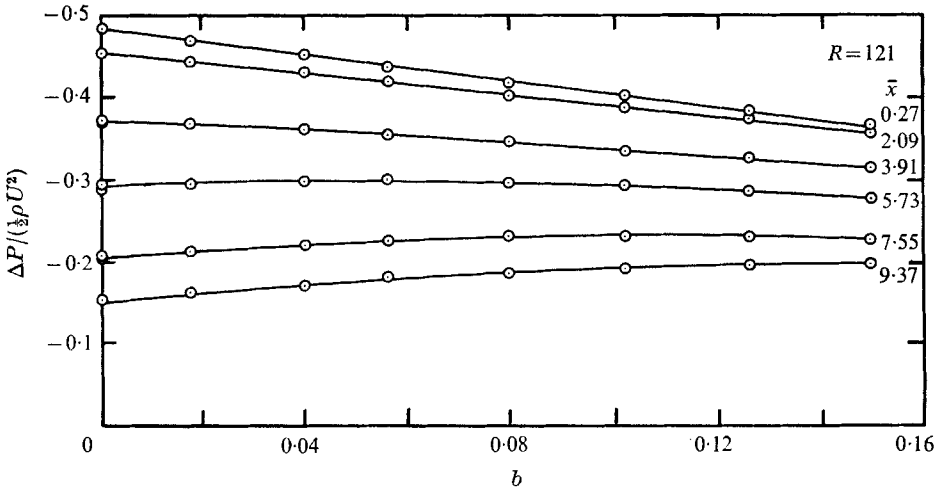

FIGURE 14. The effect of bleed rate on the pressure coefficient along the horizontal base of the model, $R = 121$; $\bar{x} = x/d$.

length l_1 shown in figure 3. This is equivalent to Pan's (1967) choice for the backward-facing step in the limit as $R \to \infty$, and yields the reduced plot of figure 17. Clearly, for $b \equiv 0$, the rate of recovery of $\hat{p}$ with $\hat{x}$ ($\equiv x/l_1$) is independent of R as expected. In contrast, for non-zero bleed rates, the appropriate length scale for normalizing the streamwise distance is difficult to select, since the closed

streamline region occupies only a portion of the near-wake which itself is apparently open-ended and thus, strictly speaking, of infinite spanwise extent. A somewhat arbitrary choice, which yields a first approximation valid for $b \ll O(1)$, is simply the wake length measured at the same R with $b \equiv 0$. Pres-

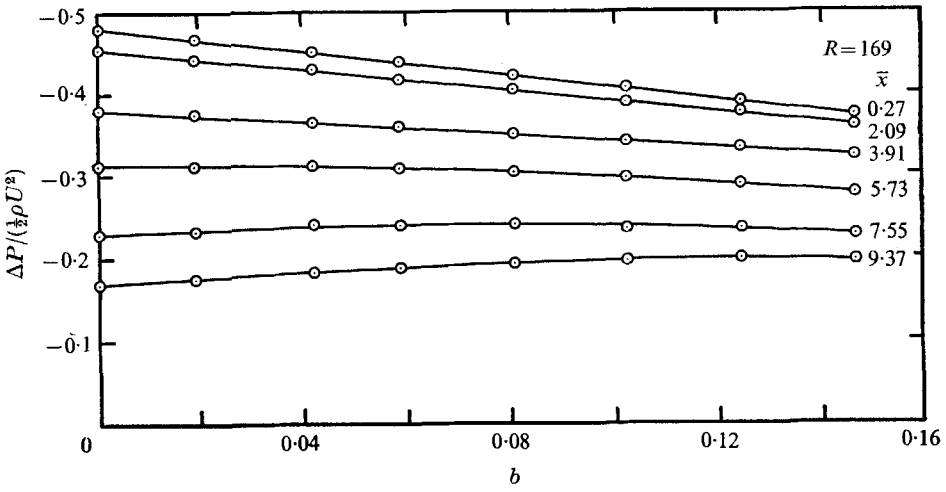

FIGURE 15. The effect of bleed rate on the pressure coefficient along the horizontal base of the model, $R = 169$; $\bar{x} = x/d$.

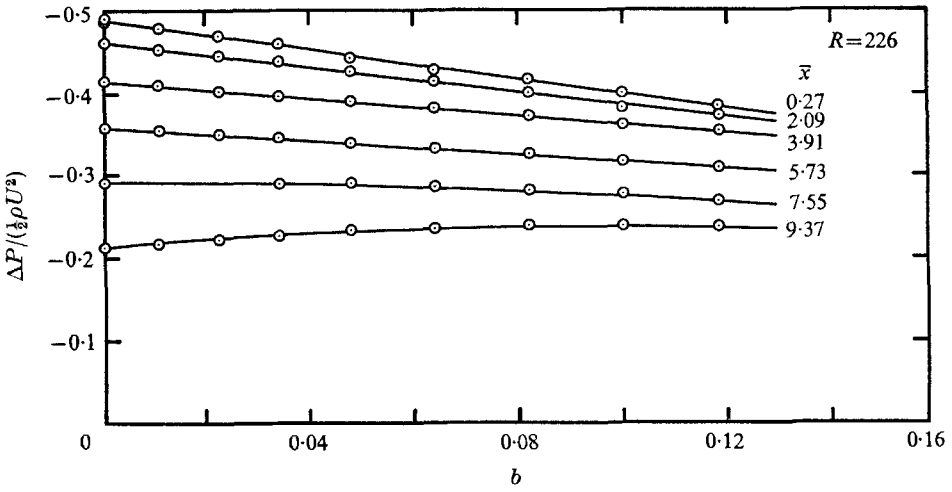

FIGURE 16. The effect of bleed rate on the pressure coefficient along the horizontal base of the model, $R = 226$; $\bar{x} = x/d$.

sure profiles so determined from the best fit curves of figures 13–16 are shown in figures 18–20 which correspond, respectively to $b = 0{\cdot}04$, $0{\cdot}08$ and $0{\cdot}12$.

Considering the approximation involved in normalizing the streamwise distance, these reduced profiles exhibit surprisingly little scatter even for $b = 0{\cdot}12$ where any resultant discrepancies should be the most severe. Clearly,

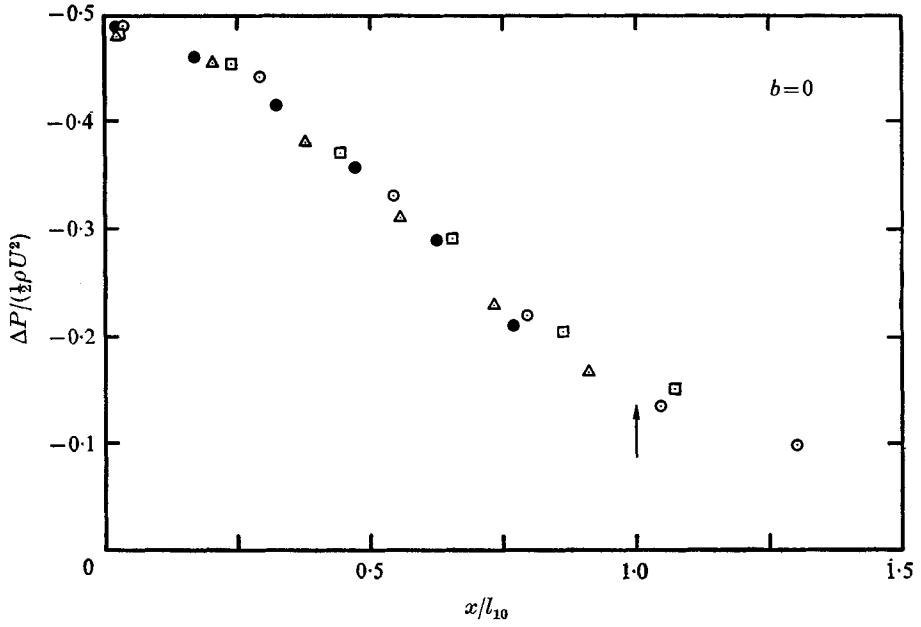

FIGURE 17. The pressure coefficient variations along the horizontal base of the model in the stretched co-ordinate x/l_{10} for $b = 0$. ⊙, $R = 86$; ⊡, $R = 121$; △, $R = 169$; ●, $R = 226$.

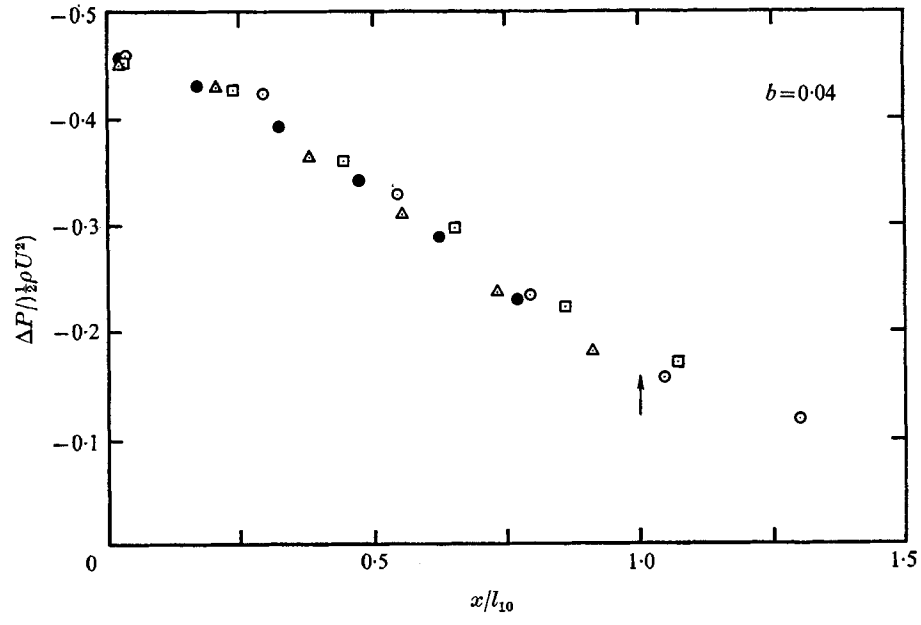

FIGURE 18. The pressure coefficient variations along the horizontal base of the model in the stretched co-ordinate x/l_{10} for $b = 0{\cdot}04$. ⊙, $R = 86$; ⊡, $R = 121$; △, $R = 169$; ●, $R = 226$.

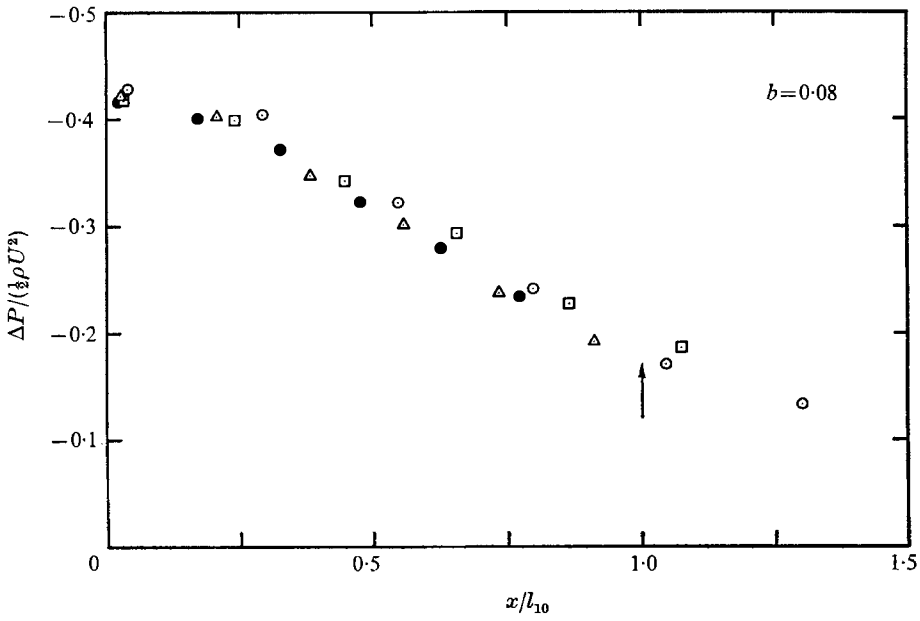

FIGURE 19. The pressure coefficient variations along the horizontal base of the model in the stretched co-ordinate x/l_{10} for $b = 0{\cdot}08$. ⊙, $R = 86$; ⊡, $R = 121$; △, $R = 169$; ●, $R = 226$.

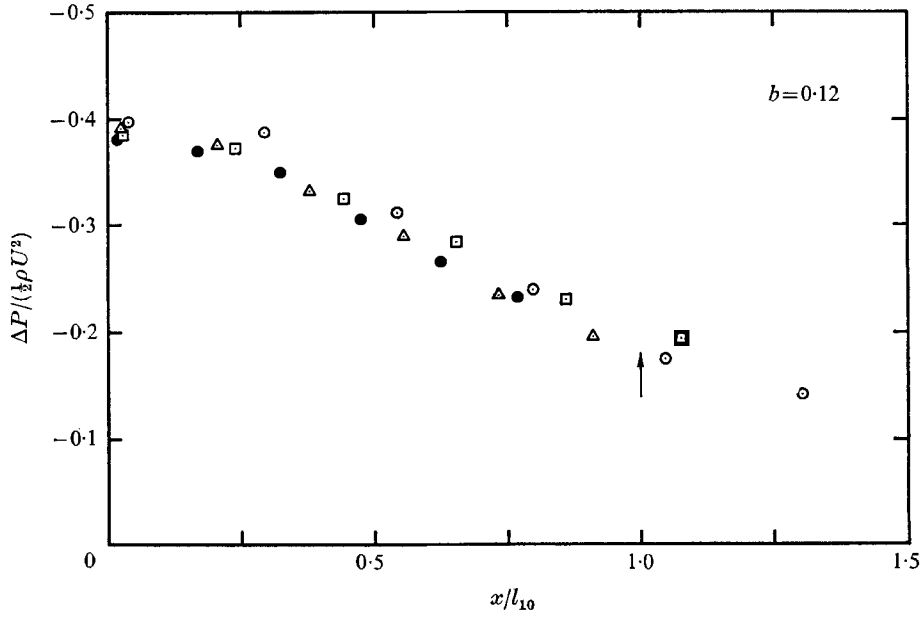

FIGURE 20. The pressure coefficient variations along the horizontal base of the model in the stretched co-ordinate x/l_{10} for $b = 0{\cdot}12$. ⊙, $R = 86$; ⊡, $R = 121$; △, $R = 169$; ●, $R = 226$.

the essential demands of the asymptotic formulation for steady separated flows at large R (cf. Acrivos *et al.* 1968) are satisfied in that the pressure coefficient at the trailing edge remains substantially negative (and constant) as R is increased, and the rate of pressure recovery relative to an 'effective' wake length is independent of R. Thus, the pressure measurements provide further evidence in support of the contention that the asymptotic formulation of the steady, high R flow, originally proposed on the basis of experimental results for steady separated wakes in the *absence* of base bleed may, in fact, remain valid even when $b \neq 0$, at least for $b \ll O(1)$.

4. Conclusions

In summary, then, the experimental results presented above seem to indicate that, in spite of considerable changes in the detailed flow patterns of the steady wake behind bluff objects, the asymptotic dependence of its basic features on Reynolds number remains qualitatively unchanged by the presence of base bleed. It appears, therefore, that the dominant properties of the recirculating region (e.g. the dependence of its length on the Reynolds number R) are relatively insensitive to the detailed flow pattern near the object but, rather, derive primarily from the presence of the shear layer that exists along the detached streamline enclosing this near-wake. This conclusion is consistent with a description of wake formation originally proposed by Chapman *et al.* (1957) and by Korst *et al.* (1956), and more recently discussed by Roshko (1967), according to which, for zero bleed, the very formation of the recirculating region behind bluff bodies is due chiefly to the flow field that results from fluid being entrained into the inner side of this shear layer, since, for any closed near-wake, the entrained fluid must eventually detrain and reverse itself in direction in order to again supply the entrainment needs of the shear layer.

This description is particularly well-suited to a discussion of the effects of base bleed on the wake structure, for, if the base bleed coefficient b is small, the amount of fluid being supplied into the near-wake is not sufficient to satisfy the entrainment needs of the shear layer along the detached streamline, and hence, for the reason stated above, a closed vortex region should form downstream. Conversely, for b sufficiently large, such a closed streamline region should be absent. This picture is consistent with Bearman's (1967) model as well as the experimental observations of the present work.

Admittedly, the apparent validity of this entrainment-detrainment mechanism as the cause of the formation of the standing eddies is not, in itself, sufficient to ensure the development of a unique model for the high Reynolds number flow, since additional assumptions need to be introduced regarding the variation with R of such basic parameters as the width of the closed streamline region and the streamwise pressure profile in the wake. In this regard, it should be noted that the calculation of the base pressure coefficient by Chapman *et al.* (1957), while leading to a reasonable value for $\hat{p}_{\text{base}}$, is based on an inviscid analysis and an assumed qualitative pressure distribution in the wake which is not only inconsistent with that of the Acrivos *et al.* (1965) theoretical model referred to previously,

but differs fundamentally from the experimentally determined profiles reported here and in (1968) by the authors. Nevertheless, the fact that this basic entrainment mechanism seems to account qualitatively for the observed flow patterns in the presence of base bleed and is consistent with the apparent dominance of the wake structure by the separated shear layers, should be helpful in arriving at a better understanding of flow phenomena involving separation and in developing a completely self-consistent theoretical model for the high Reynolds number case.

This work was supported in part by grants from the National Science Foundation and by the Petroleum Research Fund administered by the American Chemical Society; L. G. L. was further supported by a National Science Foundation graduate fellowship.

REFERENCES

ACRIVOS, A., SNOWDEN, D. D., GROVE, A. S. & PETERSEN, E. E. 1965 The steady separated flow past a circular cylinder at large Reynolds numbers. *J. Fluid Mech.* **21**, 737.

ACRIVOS, A., LEAL, L. G., SNOWDEN, D. D. & PAN, F. 1968 Further experiments on steady separated flows past bluff objects. *J. Fluid Mech.* **34**, 25.

BEARMAN, P. W. 1967 The effect of base bleed on the flow behind a two-dimensional model with a blunt trailing edge. *Aero. Quart.* **18**, 207.

CHAPMAN, D. R., KUEHN, D. M. & LARSON, H. K. 1957 Investigation of separated flows in supersonic and subsonic streams with emphasis on the effect of transition. *NACA* TN 3869. (Also *NACA* Rep. 1356.)

GROVE, A. S., SHAIR, F. H., PETERSEN, E. E. & ACRIVOS, A. 1964 An experimental investigation of the steady separated flow past a circular cylinder. *J. Fluid Mech.* **19**, 60.

KORST, H. H., PAGE, R. H. & CHILDS, M. E. 1955 A theory for base pressures in transonic and supersonic flow. University of Illinois, Engr. Exp. Sta., Mech. Engr. Dept., TN 392–2.

LEAL, L. G. 1969 A study of steady, closed streamline flows at large Reynolds number. Ph.D. Dissertation, Stanford University.

NASH, J. F. 1962 A review of research on two-dimensional base flow. *A.R.C.* R & M. 3323.

PAN, F. 1967 On closed streamline flows. Ph.D. Dissertation, Stanford University.

ROSHKO, A. 1967 A review of concepts in separated flow. Lecture presented at Canadian Congress of Applied Mechanics, Centennial Year 1967. Université, Laval Québec.

WOOD, C. F. 1967 Visualization of an incompressible wake with base bleed. *J. Fluid Mech.* **29**, 259.

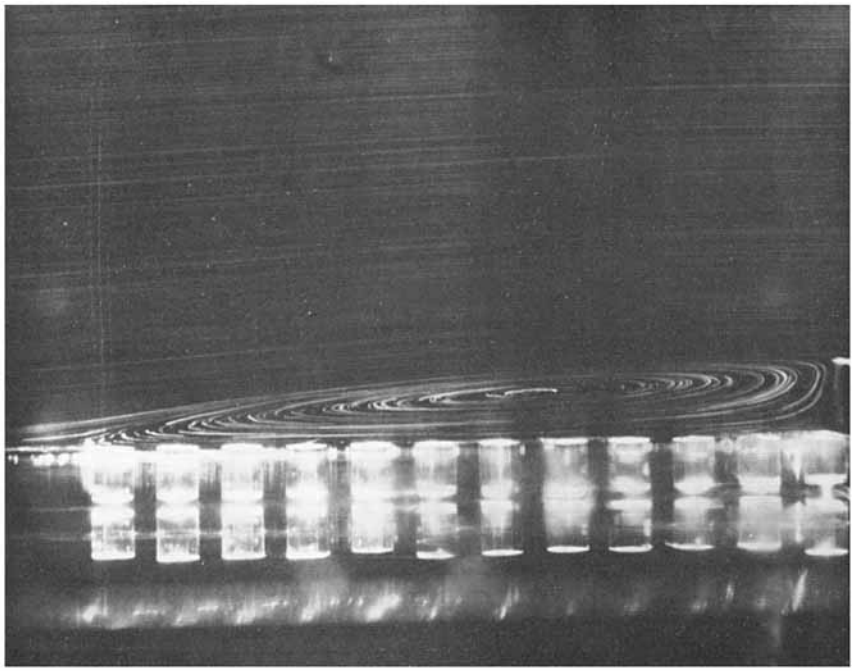

(*a*)

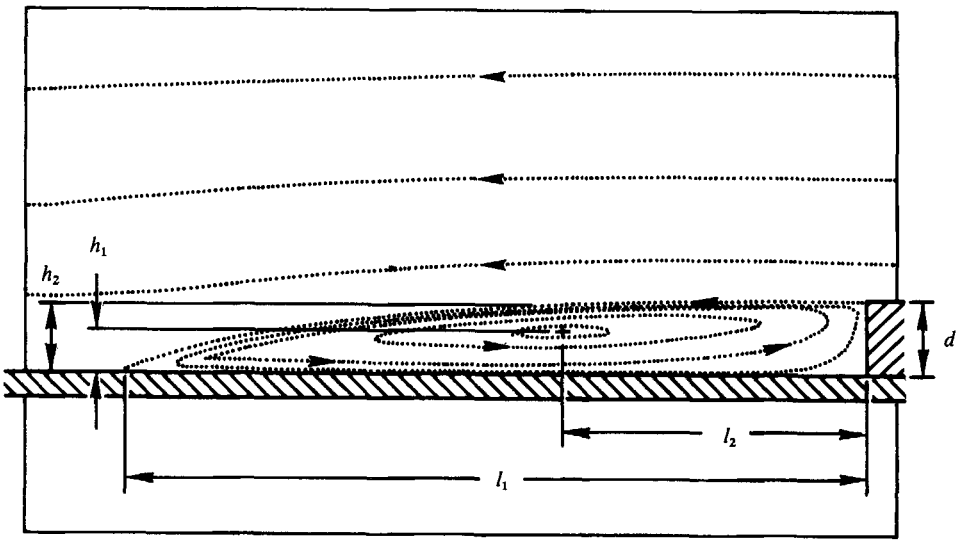

(*b*)

FIGURE 3. (*a*) A typical streamline pattern for flow in the near-wake (R = 190). (*b*) A schematic diagram of the near-wake flow field.

(*a*)

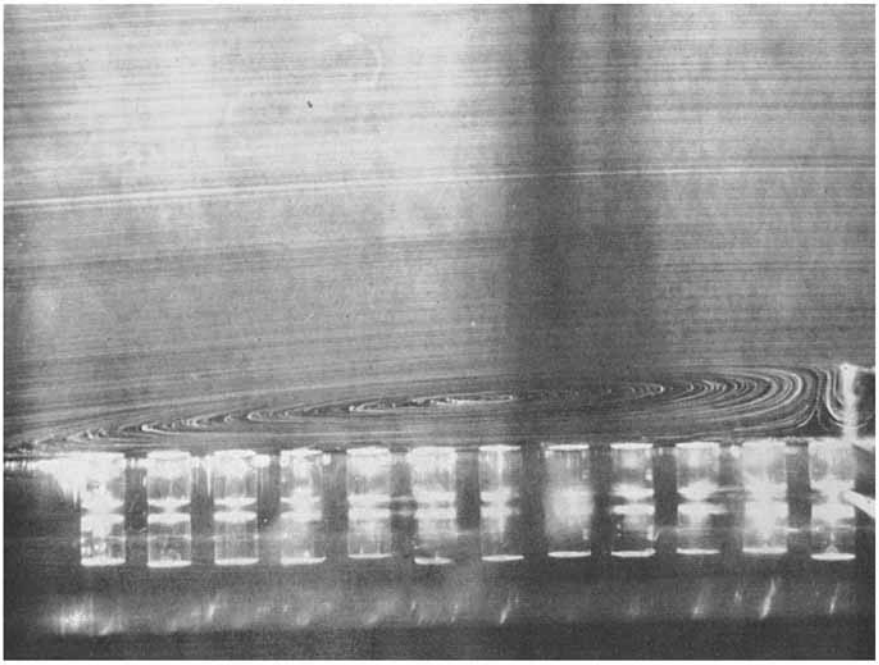

(*b*)

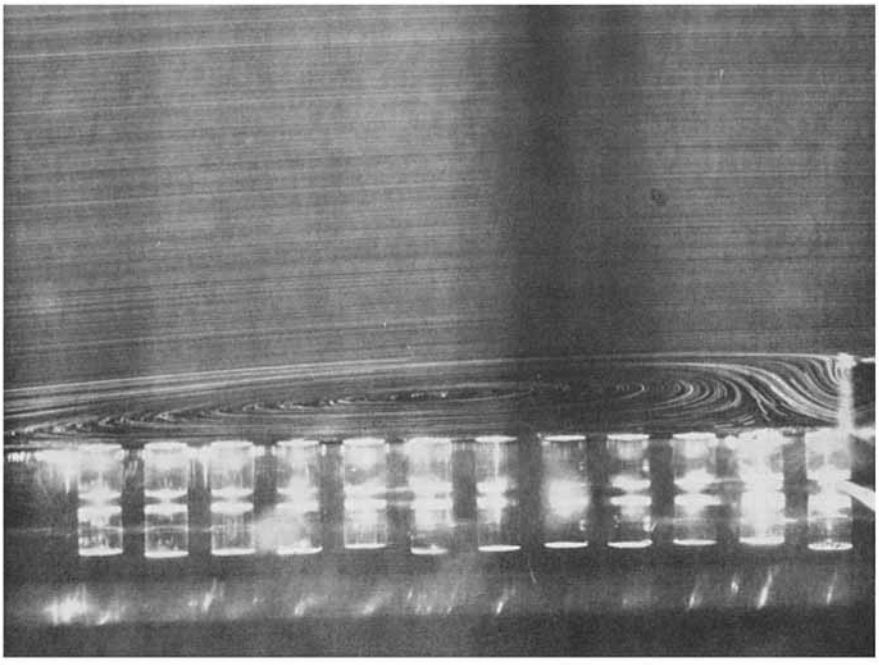

FIGURE 7. (*a*) A typical streamline pattern for $b = 0{\cdot}010$, $R = 260$, (*b*) $b = 0{\cdot}038$, $R = 260$, plate 2; (*c*) $b = 0{\cdot}059$, $R = 260$, plate 3; (*d*) $b = 0{\cdot}080$, $R = 260$, (*e*) a schematic diagram of the flow field for $b = 0{\cdot}080$, $R = 260$, plate 4.

(*c*)

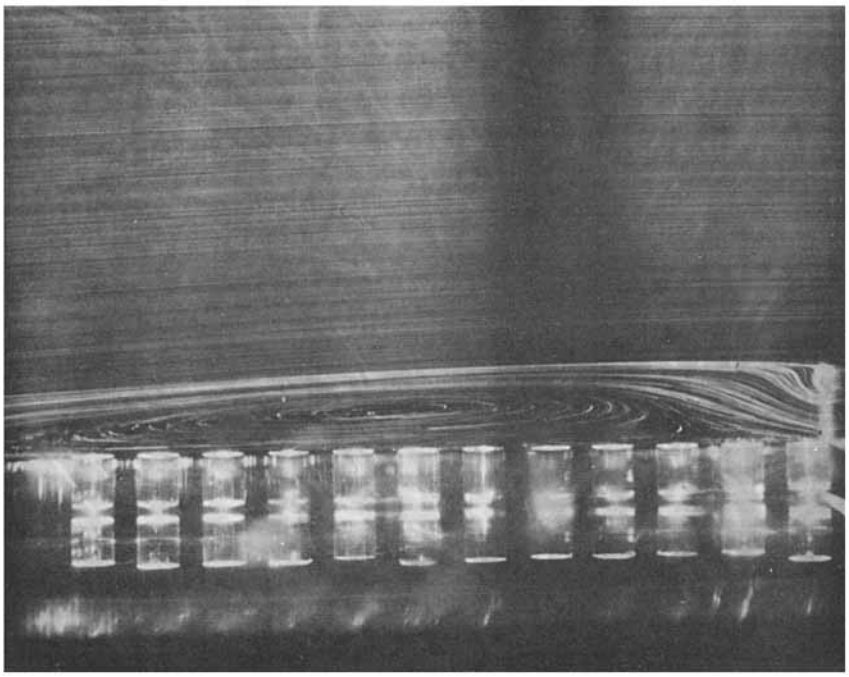

FIGURE 7. For legend see plate 2.

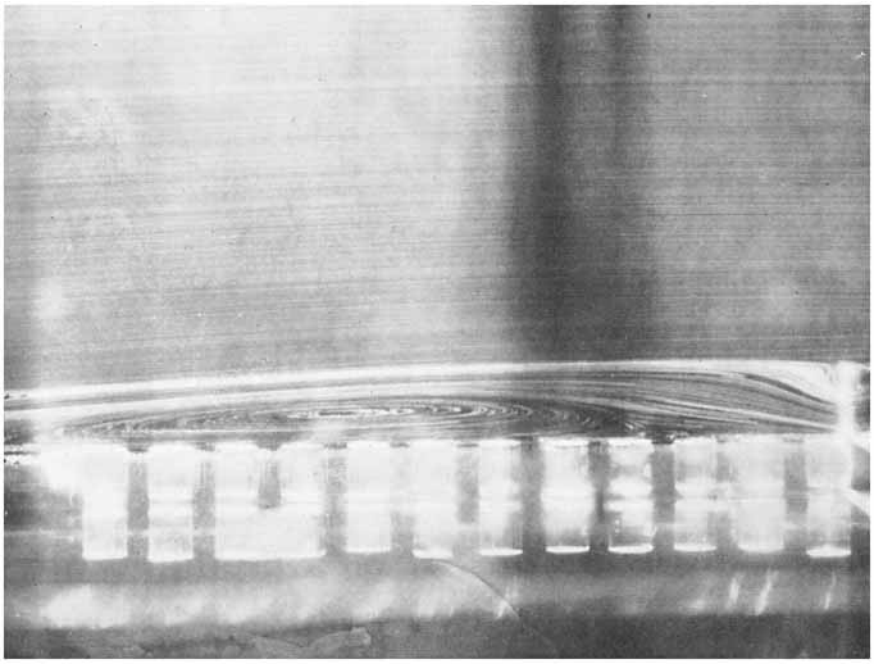

(*d*)

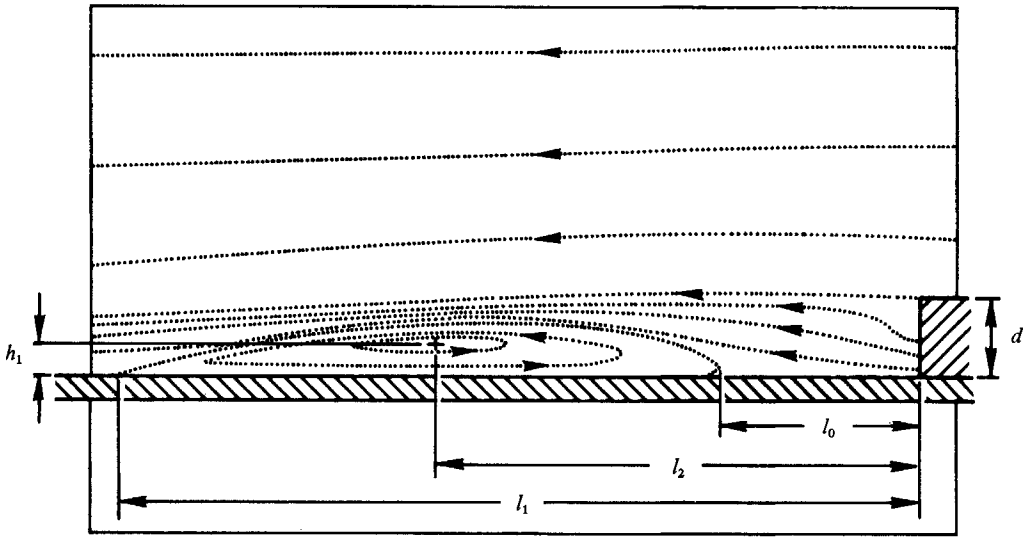

(*e*)

FIGURE 7. For legend see plate 2.